

An estimation for the 4γ branching ratio of positronium using $\text{LaBr}_3\text{:Ce}$ scintillator detectors

S Johnson^{1,2}, T Leadbeater¹ and P Jones²

¹ Department of Physics, University of Cape Town, Private Bag X3, Rondebosch, 7701, South Africa

² Department of Subatomic Physics, iThemba LABS, PO Box 722, Somerset West, 7129, South Africa

E-mail: sjohnson@tlabs.ac.za

Abstract. An approximation for the branching ratio of the four-photon decay of parapositronium ($\text{BR}_{4\gamma}$) was measured using a multi-gamma-ray spectrometer. For the first time in such measurements, the spectrometer consisted of an array of eight identical $\text{LaBr}_3\text{:Ce}$ scintillator detectors, each of which combines good energy resolutions (5% and 10% at 511 keV for the signals from the eighth dynode and anode of the photomultiplier tube, respectively) with an excellent timing resolution (~ 300 ps). Through simplifying assumptions that neglected the background corrections and efficiency normalisations for each of the 2γ and 4γ decays, a first order approximation of $\text{BR}_{4\gamma}$ was determined as the ratio between measured 4γ events ($N_{4\gamma}$) and measured 2γ events ($N_{2\gamma}$), such that $\text{BR}_{4\gamma} \sim \frac{N_{4\gamma}}{N_{2\gamma}} = 4.8 (19) \times 10^{-7}$. This measured value of $\text{BR}_{4\gamma}$ differs from previous measurements and accepted literature values by a factor of 3.

1. Introduction and background

Positrons (e^+) are the positively-charged anti-particles of electrons (e^-). Due to the prevalence of electrons in matter, free positrons are often not observed to exist for prolonged periods of time (since they quickly undergo annihilation). Following emission from a decay, a positron travelling through a medium will undergo a series of collisions with bound electrons, causing it to thermalise. Once sufficiently thermalised, the positron will undergo either one of two processes: direct annihilation with an electron of opposing spin, or it will form an exotic atom known as positronium (Ps). Ps is a quasi-stable system consisting of an electron and a positron. After a finite period of time, the two particles annihilate to produce an even or odd number of gamma-rays (depending on the relative spin states of each particle, as well as the governing energy, momentum, and charge conservation laws). Similar to that of hydrogen, the ground state of Ps has two varieties: parapositronium (p-Ps), which is a singlet state with total spin $S = 0$, and orthopositronium (o-Ps), which is a triplet state with total spin $S = 1$. The Ps state can be considered non-relativistically as the product of an orbital wave function and a spin vector given as,

$$\Psi_{n,l,m}(\mathbf{r})|S, S_z\rangle. \quad (1)$$

The orbital wave function in Equation (1) is the wave function of the hydrogen atom (with the electron mass replaced by the reduced mass of the e^+e^- pair), where n , l , and m are the usual principle ($n \in \mathbb{Z} \leq 0$), orbital ($0 \leq l < n - 1$) and magnetic ($m \leq l$) quantum numbers,

respectively. The spin vectors are linear combinations of products of those of the individual particles, of which there are four possible:

$$\begin{aligned}
 |S = 1, S_z = 1\rangle &= |\uparrow\rangle|\uparrow\rangle \\
 |S = 1, S_z = 0\rangle &= \frac{1}{\sqrt{2}} (|\uparrow\rangle|\downarrow\rangle + |\downarrow\rangle|\uparrow\rangle) \\
 |S = 1, S_z = -1\rangle &= |\downarrow\rangle|\downarrow\rangle \\
 |S = 0, S_z = 0\rangle &= \frac{1}{\sqrt{2}} (|\uparrow\rangle|\downarrow\rangle - |\downarrow\rangle|\uparrow\rangle)
 \end{aligned} \tag{2}$$

The first three expressions describe the possible spin states of o-Ps (triplet), while the last expression describes the spin state of p-Ps (singlet). The selection rule that governs the e^+e^- annihilation [1, 2] is particularly important in understanding the decay modes of Ps. As a direct consequence from the selection rule and the energy, momentum, and charge conservation laws, it can be shown that p-Ps must decay into an even number of photons (two or more), while o-Ps must decay into an odd number (three or more). This is shown succinctly by Harpen [3].

The ultimate aim of this study is to demonstrate the measurement feasibility of the four photon branching ratio of p-Ps using an array of eight identical $2 \times 2''$ Lanthanum Bromine (LaBr₃:Ce) detectors. For these measurements, locally-produced ²²Na sources of various activities were used as positron emitters. It should be noted that ²²Na has a β^+ decay branching ratio of 90.3% [4], which makes it a suitable candidate for producing Ps.

2. Experimental set-up

2.1. Detector assembly

Measurements of the gamma radiation emitted from ²²Na radioactive sources of various activities were performed with the gamma-ray spectrometer. The gamma-ray spectrometer (see Figure 1) consisted of an array of eight LaBr₃:Ce (5%) detectors (labelled as D1-D8), which were arranged in a planar geometry. These detectors were manufactured by Saint-Gobain, and each consists of a $2 \times 2''$ LaBr₃:Ce scintillation crystal lattice which is attached to a Hamamatsu R2083 PMT. A ²²Na source was placed symmetrically at the centre of the detector array, such that it was equidistant at 12 cm from the face of each detector. The source was placed on a plastic stand, which ensured that it was situated in the same plane as the centre of each detector. Based on the cylindrical geometry of each detector, and the equidistant source-to-detector distance, the solid angle subtended between the source and each detector was determined to be 1.0838 (1)% of 4π steradians. Due to the symmetry of the set-up and isotropic nature of the source, the accumulative solid angle for the eight-detector system is 8.671 (3)% of 4π steradians.

2.2. Electronics and data acquisition system

As seen in Figure 1, the electronics (including the high voltage (HV) supply, the XIA Pixie-16 module and the CPU) were all housed in a crate and NIM bin. Each detector was powered by an HV power supply, and the detectors photomultiplier tube (PMT) anodes were integrated with a model 474 ORTEC pre-amplifier to provide the signals. The operating voltages for each detector were chosen such that the detectors were gain-matched, and the data was then re-binned post-acquisition through energy calibration. The signals generated at the anode (*fast signal*) and eighth dynode (*slow signal*) of the PMT were pre-amplified, and the resulting output signals were transmitted to the XIA Pixie-16 module using RG175/lemo connectors and RG58 cables, respectively. The XIA Pixie-16 module is a 16-channel digital signal processor which samples the waveform data at 500 MHz [5]. Each of the 16 channels of the Pixie-16 module can be operated independently for data acquisition. Each channel is gated using a Channel Gate Input which

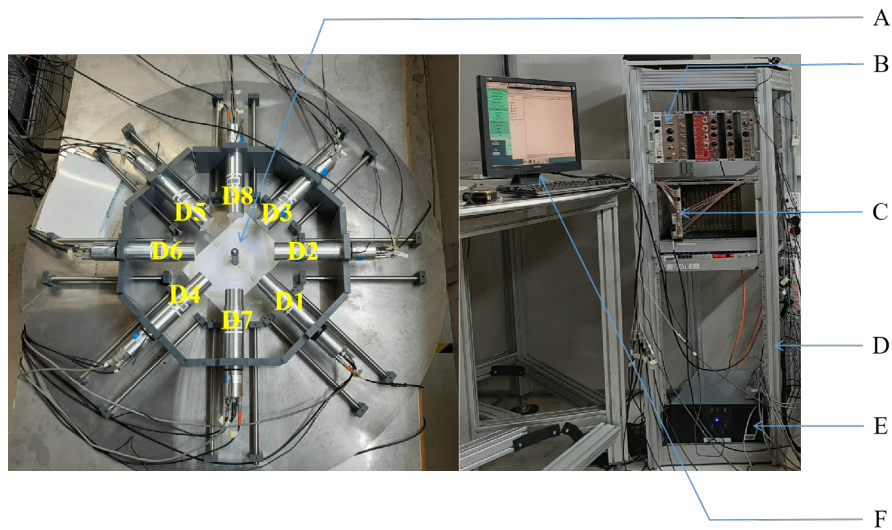


Figure 1. Eight LaBr₃:Ce detectors (D1-D8) are situated in a planar geometry. The associated electronics of the detector system are also shown. (A = ²²Na source, B = High voltage supply, C = Pixie-16, D = Crate and NIM bin, E = CPU and F = PC display).

ranges from 0-15. Each of the slow signals of detectors D1-D8 respectively, were connected to channels 0-7. Each of the fast signals of detectors D1-D8 respectively, were connected to channels 8-15. The digital signal processing (DSP) parameter settings for both the slow and fast signals were selected such that the measured energy resolutions were minimised to 5% and 10% at 511 keV for each detector, respectively. The software used for the data acquisition was the Multi Instance Data Acquisition System (or MIDAS) [6, 7]. MIDAS was able to access all of the recorded data from the hardware electronics through a single Peripheral Component Interconnect (PCI) bridge (PXI-8360). The data was recorded in list-mode and written to network storage for offline analyses. Each recorded event consisted of an event ID, timestamp (48-bit), CFD time (16-bit), and (calibrated) energy (16-bit) [5]. The measurement had an accumulative run time of 5.16×10^6 s, which is comparable to the run time of similar experiments performed by Yang *et al.* (2.02×10^7 s [1]) and Vetter & Freedman ($9.45 (1) \times 10^5$ s [8]). There were approximately 4.85×10^{11} total events (~ 12.5 TB of data) recorded at an average acquisition rate of 2.4 MB/s.

3. Data processing, analyses and results

3.1. Data reduction

Due to the large amount of data acquired during the measurement process, a filtering method was a necessary implementation. The object of the data reduction is to identify the events corresponding to both two and four photon decays, and separate each from the background events. The sorting code for the data defines the energy (E_c) and time (T_c) windows that were used to filter between various detected interactions. These windows act as logical filters which allow for the data to be categorised with specific energy and timing requirements. Specifically, the two filtering conditions that all potential Ps annihilation events must pass include:

- the sum energy of the detected photons in the event must sum to 1022 keV (so that events correspond to the real mass of the annihilating e^+e^- pair). The sum energy window E_c is set such that $|\sum_{i=1}^n E_i - 1022 \text{ keV}| < E_c = 80 \text{ keV}$.
- the detected photons must be detected in coincidence within a time window $T_c = 2 \text{ ns}$ i.e. the arrival times of each photon must occur within 2 ns of detection.

The width values for E_c and T_c for each detector in the detector array were selected such that the number of accepted 4γ events are maximised, while minimising background events from accidental interactions. These widths correspond to approximately 7σ of their respective peaks with a confidence level limit greater than 99%.

3.2. Multiplicity spectra

Figure 2 shows the multiplicity plots (T_c -gated and T_c - E_c -gated) that were generated through a data sorting code. The sorting code runs through each pair of detectors to determine whether the recorded events meet the timing and/or energy requirements defined by E_c and T_c . When sorting the data, the T_c -gated plot only applies the T_c filtering condition, while the T_c - E_c -gated plot applies both the T_c and E_c filtering conditions. A typical run through the sorting code to generate the multiplicity spectra is summarised below:

- The time difference between events in detectors j and $k \geq j + 1$ is determined such that the time difference peak is centred at some constant offset $t > 0$ (which is later set to 0 ns).
- If the time difference lies within the pre-defined time window T_c , a counter (denoted m_1) is incremented by 1. As the sorting code runs through each pair of detectors, m_1 will therefore be incremented by the number of detector pairs which have events measured in coincidence.
- The events in each detector j and k are checked for whether they correspond to the annihilation photon energy. If they lie within the energy window E_c , then a separate counter (denoted m_2) is incremented by 1. m_2 will be incremented by the number of detector pairs which have events corresponding to both the timing and energy requirements.
- After the sorting code has run through each pair of detectors, the values of m_1 and m_2 are binned separately, which generates two different multiplicity plots. The plot that bins m_1 values (T_c -gated plot) shows the multiplicity for coincident gamma-ray events, while the plot that bins m_2 (T_c - E_c -gated plot) shows the multiplicity for coincident events measured at the energy of the annihilation photon.
- This algorithm is repeated until all of the recorded data is processed.

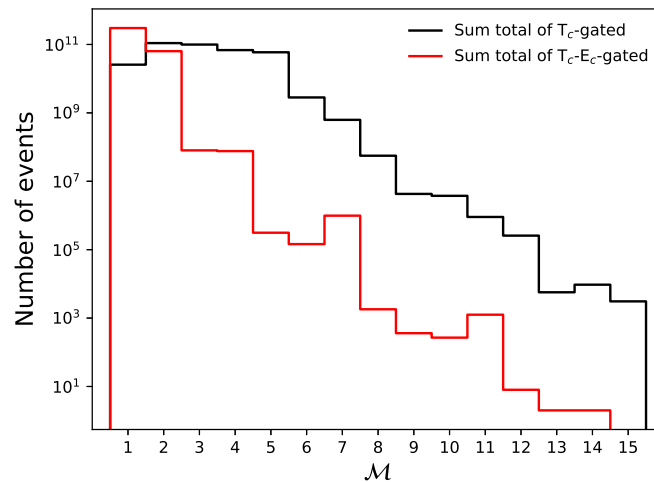


Figure 2. \mathcal{M} is shown for the contributions of both the T_c -gated (black), and T_c - E_c -gated (red) spectra. T_c -gated shows the filtered data using the time window $T_c = 2$ ns, while T_c - E_c -gated shows the filtered data using both the energy and time windows $E_c = 80$ keV and $T_c = 2$ ns.

Clearly the sorting code sorts measured events into detector pair multiplicities (which is denoted as \mathcal{M} in Figure 2). As such, the nature of this sorting allows for the use of the binomial formula,

$$\binom{n}{k=2} = \frac{n!}{k!(n-k)!} = \frac{n!}{2(n-2)!}, \quad (3)$$

where $k = 2$ because the code sorts the events into multiplicities of detector pairs. Equation (3) provides a relation between the number of detectors that detected an event to the bin number \mathcal{M} in which the event was placed. Hence, the case of $n = 2$ would correspond to the number of counts recorded between any two detectors, and is calculated as $\binom{2}{2} = 1$. This shows that a pair of detectors has a multiplicity of $\mathcal{M} = 1$, and so all 2γ events will be recorded in bin number 1 of the T_c - E_c -gated plot. Excluding accidental background interactions, the majority of these 2γ events ($\sim 60\%$ for most materials [9]) are resultant from direct annihilation, while the rest arise from the 2γ decay of Ps. For ease of reference, the counts corresponding to $\mathcal{M} = 1$ in the T_c - E_c -gated plot are denoted as $N_{2\gamma} = 3.02 (21) \times 10^{11}$. For the case of four detectors, $n = 4$, and so Equation (3) becomes $\binom{4}{2} = 6$. So the case of four detectors has a multiplicity of $\mathcal{M} = 6$, and hence, all possible 4γ events (the majority of which are from the 4γ decay of Ps) will be recorded in bin number 6 of the T_c - E_c -gated plot. For ease of reference, the counts corresponding to $\mathcal{M} = 6$ in the T_c - E_c -gated plot are denoted as $N_{4\gamma} = 1.45 (55) \times 10^5$. The values of $N_{2\gamma}$ and $N_{4\gamma}$ are used for the 4γ branching ratio calculation in the following section. The counts corresponding to other \mathcal{M} values are resultant from other detector multiplicities that are not of interest to this work. There are two types of uncertainties considered for the counts of the multiplicity spectra in Figure 2. These include the uncertainty from the coincident counting of event multiplicities (statistical), and the selection of window filter values for E_c and T_c (systematic). The statistical uncertainty was found to be several orders of magnitude smaller than the systematic uncertainty. It should also be mentioned that the relatively long measurement period of this work (~ 1433 hours) reduces the statistical noise of the measurement, and hence, the systematic uncertainty is the main contribution to the uncertainties shown in $N_{2\gamma}$ and $N_{4\gamma}$.

3.3. Calculations and discussion

Vetter & Freedman [8] determined the 4γ branching ratio of p-Ps (denoted $\text{BR}_{4\gamma}$) using,

$$\text{BR}_{4\gamma} = \frac{(N_{4\gamma} - B_{4\gamma})\epsilon_{2\gamma}}{N_{2\gamma}\epsilon_{4\gamma}}. \quad (4)$$

where $N_{n\gamma}$ represents the number of $n\gamma$ events observed, $B_{4\gamma}$ is the expected number of 4γ background events, and $\epsilon_{n\gamma}$ is the detection efficiency of the detector array for $n\gamma$ annihilations. Equation (4) is derived from the ratio between the number of detected 4γ events with the number of detected 2γ events (both normalised with their respective detection efficiencies). Lastly, the correction term $B_{4\gamma}$ accounts for the accidental detections of 4γ background events. In the previous section, the values for $N_{2\gamma}$ and $N_{4\gamma}$ were highlighted as key results from the T_c - E_c -gated plot of Figure 2. In order to complete the calculation of Equation (4), values for $B_{4\gamma}$, $\epsilon_{2\gamma}$ and $\epsilon_{4\gamma}$ must be estimated. From previous measurements of $\text{BR}_{4\gamma}$, Adachi *et al.* [10], Yang *et al.* [1], and Vetter & Freedman [8] evaluated these quantities (or similar) by performing Monte Carlo detector simulations for their respective experiments. Such simulations are beyond the scope of the current work, and is suggested as follow up. However, a suitable estimate for $\text{BR}_{4\gamma}$ can be obtained using this work's measured values for $N_{2\gamma}$ and $N_{4\gamma}$. At its most fundamental level, Equation (4) is the ratio between the number of detected 4γ events with the number of detected 2γ events. Neglecting the secondary considerations of 4γ background subtraction and efficiency normalisations, a suitable 'first order' approximation for $\text{BR}_{4\gamma}$ can be obtained as,

$$\text{BR}_{4\gamma} \sim \frac{N_{4\gamma}}{N_{2\gamma}} = 4.8 (19) \times 10^{-7}. \quad (5)$$

While this result is not a true measurement of $BR_{4\gamma}$, it does seem to be a fairly promising estimation. The accepted value for $BR_{4\gamma}$ is given by $BR_{4\gamma,theory} = 1.4388 (21) \times 10^{-6}$ [11], which is a factor of 3 larger than the estimate. From similar measurements of previous publications, Vetter & Freedman [8] found $\frac{N_{4\gamma}}{N_{2\gamma}} \sim 5 \times 10^{-9}$, while Adachi *et al.* [10] found $\frac{N_{4\gamma}}{N_{2\gamma}} \sim 5 \times 10^{-8}$. The discrepancies observed between these ratios are expected. The experimental set-up of this work and each of the aforementioned publications differ significantly (different detectors, detector geometries, and radioactive sources), which would suggest that the 2γ and 4γ detection efficiencies for each set-up would then also likely differ. Therefore, different measurements for $\frac{N_{4\gamma}}{N_{2\gamma}}$ will be found depending on the experimental set-up. As a consequence, there is no apparent method to quantify the quality of the $BR_{4\gamma}$ estimation from this work.

4. Summary and further work

The aim of this study was to demonstrate the measurement feasibility of the four photon branching ratio of p-Ps (denoted $BR_{4\gamma}$) using the experimental set-up described in Section 2. A complete calculation of $BR_{4\gamma}$ was not performed, since key factors from Equation (4) (specifically $B_{4\gamma}$, $\epsilon_{2\gamma}$ and $\epsilon_{4\gamma}$) were not evaluated. However, the key results of $N_{2\gamma}$ and $N_{4\gamma}$ were obtained through the generation of multiplicity spectra that allowed for the separation of the data into a binned distribution. The ratio between the values of $N_{4\gamma}$ and $N_{2\gamma}$ allowed for an order of magnitude to be estimated for $BR_{4\gamma}$ given by,

$$BR_{4\gamma} \sim 5 (2) \times 10^{-7}.$$

This estimation was compared to the accepted value, and was found to differ by a factor of 3. The most obvious limitation of this work is the lack of a final measurement result for $BR_{4\gamma}$. An improvement, therefore, would be to evaluate the factors $B_{4\gamma}$, $\epsilon_{2\gamma}$ and $\epsilon_{4\gamma}$ using Monte Carlo simulations for this work's experimental set-up. Factoring in these additional results using Equation (4) will allow for a complete calculation to be performed, and will provide a conclusive measurement of $BR_{4\gamma}$ (comparable to the literature values quoted).

References

- [1] Yang J, Chiba M, Hamatsu R, Hirose T, Matsumoto T and Yu J 1996 *Physical Review A* **54** 1952
- [2] Wolfenstein L and Ravenhall D G 1952 *Physical Review* **88** 279–282
- [3] Harpen M D 2003 *Medical Physics* **31** 57–61
- [4] Bé M M, Chisté V, Dulieu C, Mougeot X, Browne E, Chechev V, Kuzmenko N, Kondev F, Luca A, Galán M, Nichols A, Arinc A and Huang X 2010 *Table of Radionuclides (Monographie BIPM-5 vol 5)* (Pavillon de Breteuil, F-92310 Sèvres, France: Bureau International des Poids et Mesures) ISBN 92-822-2234-8
- [5] LLC X 2005 User's manual digital gamma finder (dgg) pixie-16 URL http://www.phys.utk.edu/expnuclear/LeRIBSS/Pixie16_UserManual1.0.6.pdf
- [6] Jones P 2013 ithemba labs annual report URL https://tllabs.ac.za/wp-content/uploads/pdf/annual_reports/Annual_Report_2013_small.pdf
- [7] Midas website URL <http://npg.dl.ac.uk/MIDAS/>
- [8] Vetter P A and Freedman S J 2002 *Physical Review A* **66** 052505
- [9] Castellaz P, Siegle A and Stoll H 2002 *Journal of Nuclear and Radiochemical Sciences* **3** R1–R7
- [10] Adachi S, Chiba M, Hirose T, Nagayama S, Nakamitsu Y, Sato T and Yamada T 1994 *Physical Review A* **49** 3201–3208
- [11] Vetter P A 2004 *Modern Physics Letters A* **19** 871–885